SOLAR ENERGY POTENTIAL FOR COMMERCIAL BUILDING FAÇADE RETROFIT

Edvinas Bigaila[1], Caroline Hachem-Vermette[2], Mohamed El-Sayed[2], Andreas K. Athienitis[1]
[1]Centre for Zero Energy Building Studies, Concordia University, Montreal, Quebec, Canada
[2]Faculty of Environmental Design, University of Calgary, Calgary, Canada

ABSTRACT

Retrofit of existing buildings, as an evolving field of research, represents vast possibilities in increasing the energy efficiency of buildings. Façade design plays a crucial role in the retrofit of a building, and can offer additional benefits by incorporating possibilities of energy production. In this paper a commercial building in Saskatoon (Canada) is considered for solar façade retrofit potential analysis. A retrofit methodology using solar technologies is under development and a feasibility study carried out. A Tregenza sky model is used to evaluate the design options for façade configurations with overhang and spandrel integrated photovoltaics. An integrated design approach is demonstrated and results are compared using Net Zero Energy targets and Life Cycle Analysis as main feasibility criteria. The methods employed in this paper can serve as a basis to develop a methodology of facades' retrofit in cold climate urban areas.

INTRODUCTION

The need to retrofit old buildings lies in the fact, that energy use and energy related emissions from existing building stock is dominant compared to new – energy efficient buildings (Voss, 2000). Investing in conservation and efficiency measures in old existing (and new) office buildings improve not only greenhouse gas (GHG) emission related performance and reduce energy consumption costs, but also improve tenant health and productivity, increase the value of the building which in turn create higher revenue for the building owner and/or renter (Martinez & Carlson, 2014).

A significant percentage of existing building stock in both North America and in Europe was constructed post-World War II era, which are characterized by strong structural systems, but inefficient envelopes, which as a result of abundant and cheap energy led to strong reliance on new mechanical air conditioning systems of that time, displacing the use of passive design features, like natural ventilation, daylight harvesting and solar heat retention or rejection (Lechner, 2014; Martinez et al., 2015). In Canada there are approximately 83,500 non-medical commercial office buildings covering 147.5 million square meters of floor space and having an average energy use intensity (EUI) of 333 ekWh/m^2 (NRCan-OEE, 2013). 80% of Canada's non-medical office buildings were constructed before the year 2000, which results in 79% of the total commercial building related energy use (NRCan-OEE, 2013). Approximately 57% of these buildings had not undergone any type of retrofit yet by the year 2009 (NRTEE, 2009).

Reasons for a building retrofit can range from failure of building envelope, structure or mechanical components, need for increased comfort inside the building or energy performance requirements (Voss, 2000). It is recommended by Buildings Owners and Managers Association (BOMA) to consider the low cost solutions for retrofit first, like internal equipment replacement, controls, lighting retrofits, mechanical systems, etc. (Gnanam, 2013). This approach is preferred since estimated simple payback years are between less than 2 to 12 years (Nock & Wheelock, 2010). The issue with this approach is that if the envelope is not complying with existing requirements for U-values, air tightness, glazing type, appropriate solar control, window to wall ratios, etc. defined by provincial and local requirements, the total potential energy efficiency targets for the building may be not achieved. Add to that, both commercial and residential building's energy use for heating, cooling, ventilation and lighting accounts to more than 50% of the total energy consumption in the building, which is directly linked to façade design and performance.

A high performance façade is capable of not only separating the indoor environment from outdoor, transmitting daylight and solar heat, but also assisting or replacing oversized ventilation, heating and cooling systems, adapting to changing climate conditions and generating and storing energy (Quesada et al., 2012).

This paper focuses on one aspect of this topic – it assesses the potential of solar energy system

integration with façade in a commercial building façade retrofit project in Saskatoon, Canada. An integrated energy model was developed to analyze the potential of energy saving and generation potential using façade integrated PV systems in a retrofit project.

ENVELOPE RETROFIT

Recommended basic steps for any retrofit project are (i.) ensuring the commitment from the property owner, (ii.) benchmarking the performance of the existing building, (iii.) energy auditing and assessment of the retrofit opportunities, (iv.) identifying the retrofit measures to go from existing case to required performance level, (v.) the implementation phase and (vi.) continuous monitoring to ensure the system is working as planned (Gnanam, 2013).

Design guidelines are scarce for such projects and this research study in part addresses this need. The majority of existing buildings lack proper documentation and necessary performance data. Consequently developed building models are with high uncertainty (Heo, Choudhary, & Augenbroe, 2012). Usually, a perceived optimal retrofit case is chosen by the building owner hiring engineers or contractors of relevant trades, who perform various level investigations of the building and suggesting a compromise between cost and estimated performance, which is usually done based on their expertise (Rysanek & Choudhary, 2013). Estimations are done using building energy models and in order to choose optimal retrofit approach several methodologies exist: physical modeling and optimization techniques using third-party automated programs (Christensen et al., 2006), quasi-steady-state building energy models for (usually) single zone energy balance to quickly estimate the energy performance of a larger set of retrofit options (van Dijk, Spiekman, & de Wilde, 2005) and high-fidelity surrogate models based on regression techniques (Eisenhower et al., 2012) (Rysanek & Choudhary, 2013). Existing retrofit toolkits can be empirical data driven, normative or using advanced energy tools with pre-simulated building model databases. These toolkits are usually limited to existing conventional retrofit approaches and emerging technologies are hard to evaluate, limited to geography, hard to evaluate integrated effects if multiple retrofit measures are considered and challenges with model calibration (Lee et al., 2015).

TECHNOLOGIES CONSIDERED

The use of solar systems for building retrofit application is still at an early research stage. Already, the solar systems for building heating and cooling are competitive from energy and life cycle cost point of view (Henning & Doll, 2012). The mature solar thermal and photovoltaic systems are available for building integration and were applied in number of residential, commercial and industrial projects (Bambara, Athienitis, & O'Neill, 2011), (Hastings, 1999), (Zondag, 2008). However, they have not yet become a common part of most retrofit projects. The main reasons for low adoption of solar systems for retrofit projects are higher initial costs, lack of support from local policies, low local fossil fuel prices, lack of experience from designers, installers, suppliers, lack of installed capacity to observe long term performance and determine the durability and dynamic performance of building integrated solar systems (Zhang et al., 2015).

For successful deployment of photovoltaic systems in urban areas, assessment of local solar potential and estimation of partial shading can be performed using ray-tracing algorithms to predict the performance of various energy generating technologies, including solar, in the city boundaries (Bobinson et al., 2009; Robinson et al., 2007; Sarralde et al., 2015), digital surface modeling of the urban region built with Light Detection and RANGING (LiDAR) surveys data linked to Geographical Information Systems (GIS) (Esclapés et al., 2014; Redweik, Catita, & Brito, 2013) or less complex engineering methods (Márquez-García et al, 2013), (Duffie & Beckman, 2006). A TREGENZA sky model existing in TRNYS/SketchUp (Tregenza, 1987) is used in this study to study the shading effect on façade solar system energy generation potential.

Photovoltaic panel on façade can be superimposed or integrated. Superimposed panels are installed over existing exterior cladding or other finishing and do not act as envelope component. Integrated panels act as envelope elements and can be a cold façade, hot façade or shadow device (Fuentes, 2007; Lai & Hokoi, 2015). Hot façade systems demonstrate lower electrical efficiency, since the PV modules tend to have higher temperatures at the same environmental conditions. The annual production difference depends from the type of PV cell used. For mono-crystalline cells the difference in annual energy generation output of non-ventilated hot facade is in the range of 7-13% compared to free standing or optimally ventilated PV cladding (Guiavarch & Peuportier, 2006). The heat from the PV modules can be

recovered and used in non-residential buildings for fresh air preheating purposes (Jensen, 2001), (Bambara et al., 2011), thermally driven cooling applications (Mei et al., 2006) or stored (Chen, 2013). A prefabricated panel was developed for Portuguese residential housing façade retrofit applications with possible integration of PV modules on the exterior face and demonstrated high payback times (between 4.6-6.9 years) due to integrated design approach and combined savings of both retrofit and power production (Silva et al., 2013).

Exterior shading devices are an effective way of controlling solar gains. Depending from the type of building, climate, lighting demands, façade type and architectural requirements a number of technologies are available (Kirimtat et al., 2016). Appropriate design involves optimizing for cooling, heating and light energy consumption, thermal comfort in the space and glare management (Gugliermetti & Bisegna, 2006; van Moeseke, Bruyère, & De Herde, 2007). Applying appropriate integrated design decisions and control strategies up to 45% combined annual energy demand savings were demonstrated for Canadian climate compared to no shading and passive lighting control case (Tzempelikos & Athienitis, 2007). Integration of solar energy generation technologies like PV panels or transpired solar thermal collectors on exterior shading devices can lead to additional energy generation (Maurer & Kuhn, 2012; Saranti, Tsoutsos, & Mandalaki, 2015).

PV products for non-residential retrofits were described in several studies, analyzing the integration approach, the energy balance of the solar system and the building, performance of the PV system and economic and/or environmental analysis (IEA, 2014; Voss, 2000). This work extends on the previous experiences and knowledge on solar façade design and modeling, focusing on performing integrated design approach to evaluate the solar system potential for an office building façade retrofit project in Canadian climate.

METHODOLOGY

For the analysis of the solar system potential in a retrofit application the following steps have been taken:

1. Development of a validated building model to benchmark the existing building performance and analyze conventional façade retrofit potential on the whole building scale;
2. Site solar potential estimated using Tregenza sky model implemented in SketchUp.
3. Development of an integrated perimeter zone model with optimized performance and analysis of passive façade retrofit measures and façade integrated solar system energy generation potential and effect on heat and/or cool demand and electricity consumption for lighting; Solar systems modeled: a. PV overhang, b. Vertical PV shade; c. Spandrel integrated BIPV/T; d. Roof systems were considered as well for reference.
4. Energy and life cycle analysis of south and west perimeter zones façade retrofit measures.

CASE STUDY BUILDING

The building is situated in Saskatoon, Saskatchewan State, Canada. The geographic location is 52.13^{o} North and 106.68^{o} West. The building's near-south façade has a surface azimuth angle 17.1^{o} towards west. On the near-south side of the lot there is a parking space with a possible construction site in near future. Weather file information for Saskatoon shows that the solar global horizontal irradiation ranges between 280 W/m^2 and 700 W/m^2 with 5813 HDD and 765 CDD.

The building has four stories, in addition to a basement space and shown in figure 1. The gross floor area is 6528 m^2. Total façade area is 2459 m^2, total glazing area is 857.3 m^2. The building slab is medium weight concrete construction. Exterior wall consists of porcelain enamel on steel spandrel panels and limestone facing, air gap, 20.32 cm clay "Terra Cotta" bricks, 5.1 cm mineral wool insulation and interior plaster with aluminum frame double pane glazing with air gap. Window-to-wall ratio (WWR) for south and west façade is 48%.

Figure 1: Case study building south and west facades.

Currently heating is performed with a boiler located in the basement. The air-handling unit is roof mounted with air distribution capacity of 8495 m^3/hr. The heating coil is 166 kW at 8495 m^3/hr. The capacity of direct expansion cooling coil is 28 kW.

The whole building was modeled with the EnergyPlus software (U.S. DOE, 2015) and calibrated against monthly annual electricity consumption bill with CV-

RMSE-12.63% and NMBE 4.01%, electricity power draw measured at 15 min intervals with CV-RMSE 5.13% (shown in figure below) and NMBE 1.8%, monthly natural gas consumption bill with CV-RMSE 14.72% and -1.11%. The validated model facade RSI was 0.88, glazing U value was 3.52 W/m^2-ºC with solar heat gain coefficient (SHGC) 0.62, plug loads - 7 W/m^2 and lighting density - 11.95 W/m^2.

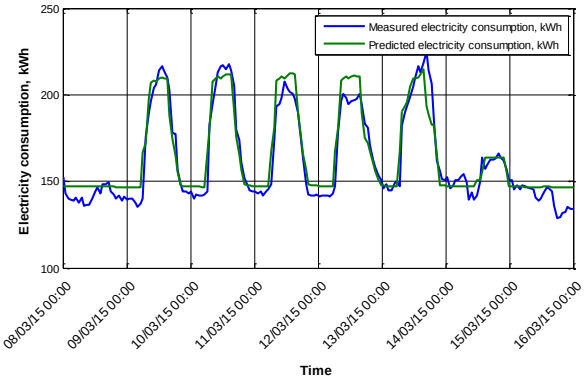

Figure 2: Measured and predicted electricity draw profile**.**

Natural gas consumption for considered year (2014-06 to 2015-05) is 86,384 m^3 which resulted in 0.95$/m^2 for heating needs. Electricity consumption was 1,493,640 kWh or 228.79 kWh/m^2, which resulted in 18.13 $/m^2. Total equivalent energy consumption of the building is 365 ekWh/m^2-yr.

The building energy use intensity was compared to Canadas' average commercial and institutional energy use determined by Natural Resources Canada (NRCan-OEE, 2013) from approximately 83,500 non-medical commercial office buildings in Canada covering 147.5 million m^2 of floor space having and average energy use intensity of 333 ekWh/m^2. Building Owners and Managers Association Building Environmental Standards (BOMA Best) is an organization which represents and supports the Canadian commercial building sector activity while promoting environmental stewardship (BOMA Canada). Based on their established office benchmarking matrix maximum (BOMA BESt low) and minimum (BOMA BESt high) points can be achieved for energy use intensity of 108 ekWhm^2-yr and 388 ekWh/m^2-yr respectively (Boma Best, 2015). The last benchmark number is obtained from a simulation study of buildings modeled according to ASHRAE 90.1-2013 requirements, which resulted an energy use intensity of 387 ekWh/m^2-yr for a medium size office (Halverson et al., 2014). The benchmark results show that the building overall performance is above Canadian average and BOMA BESt low EUI case.

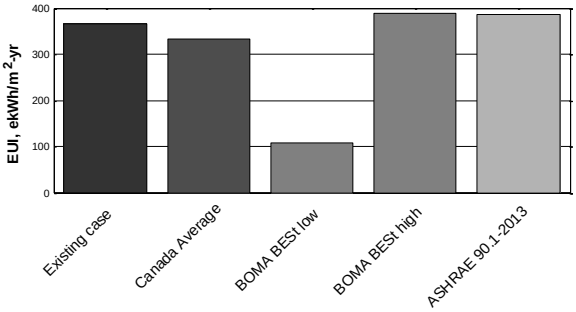

Figure 3: Building performance comparison against available benchmark levels.

RETROFIT MEASURES CONSIDERED

Façade retrofit measures and the main parameters used in the techno-economic analysis are given in the tables below. Additional insulation levels include replacement of existing steel enamel panels with new metal cladding, other materials (grits, screws and caulk), various EPS insulation levels plus 50% for labor, 5% sales tax, 10% contractor fees and 35% to take into account modeling discrepancies as a pessimistic economic scenario. Glazing replacement takes into account IGU price plus installation costs - 50% of IGU price and other materials (caulk, interior finish) - 20%. The prices are obtained from authors personal communications and quotes supplied by vendors and contractors.

Table 1: Additional insulation level costs.

Insulation level, RSI	Price, $/m^2	Redesign of south and west façade window opening, $/m^2
0.2	58	179
0.7	78	197
1.2	90	217
1.7	103	234
2.2	115	257
2.7	130	269
3.2	138	290
3.7	152	310
4.2	165	330
4.7	178	350
5.2	185	370

Table 2: Glazing replacement costs.

U, W/m^{2}ºC	SHGC	Price, $/m^2
3.52	0.62	168
3.04	0.62	188
2.89	0.5	209
2.16	0.5	229

Estimated prices for solar systems are as shown in the table below. The estimation is done based on current market prices provided by certified solar systems retailers and companies. All systems are coupled with 90% power output assurance for 10 years and 80% power output assurance for 25 years. Balance of

system components (structural, electrical, thermal or aesthetic integrity) are taken into account as additional 20% from solar component price, plus 10% market price tolerance. PV/T systems include components like circulation pumps and pipes.

Table 3: Solar system costs.

	Total purchase and delivery costs, $/m2
Overhang	212
PV shutter	309
Spandrel BIPV	248
Spandrel BIPV/T	375
Roof PV rack system	277
Roof mounted air PV/T	447

SITE SOLAR POTENTIAL

Five cases are analyzed taking into account several hypothetical building heights in front of the case study building on the other side of the street from south side (where the parking lot is currently but a future building may be built): base case is the case without any shading and hypothetical shading from building of heights 19 m, 40 m, 60 m and 80 m respectively. The lowest of these obstructions (19 m) corresponds to a building of a similar height to the analyzed building, while the highest (80 m) corresponds to the highest building according to the zoning of the City of Saskatoon.

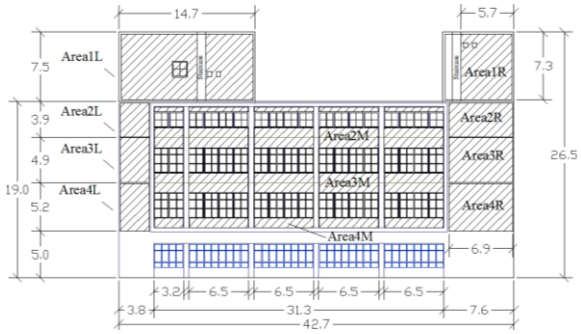

Table 4: South façade area codes.

The results show that the effect of building height is significant on the solar gains of the lower part of the façade (up to 55% annual solar gain reduction from 80 m height building). The least affected areas are the towers on the north side of the building (up to 20% annual solar gain reduction from 80 m height building). Other results are shown in the figure below.

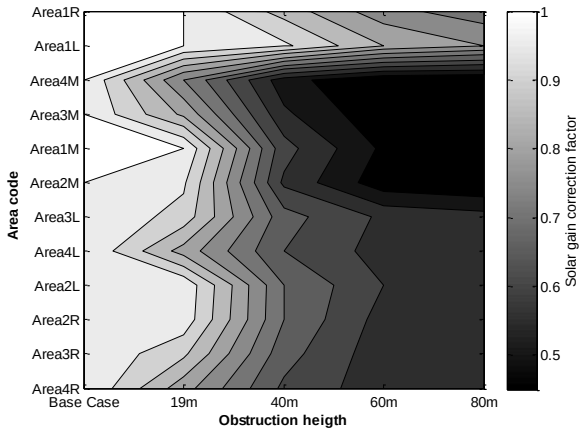

Figure 4: South façade solar potential map.

MATHEMATICAL MODELS

BIPV/T SYSTEM MODEL

A photovoltaic panel installed over the structural and insulating layer of wall or roof, thus creating a cavity, transforms a standard element into a BIPV/T façade or roof. The cavity must be either naturally or mechanically ventilated since temperature of silicon and thin-film PV cells affects the efficiency of the sunlight conversion into electricity negatively with increasing temperatures in the range of -0.035 to -0.496 $\%^{o}C^{-1}$ depending on the cell type used in PV modules (Mattei et al., 2006). The removed heat from the PV panels can be used for various low grade heat applications. The BIPV/T is thermally linked to the building as well.

The model is a quasi-steady state based on energy balance of a solar air based flat plate collector. The solar absorber is the exterior opaque plate, which is the PV panel in this case. The energy balance is described by Luis Candanedo (Candanedo et al., 2010).

To estimate the convective heat transfer in BIPV/T air cavity Nu numbers are used as follows. If Reynolds number is 0, then the Nu number correlation for natural convection heat transfer is utilized. This case applies for cold BIPV façade or the case when BIPV/T fan is OFF:

$$Nu = 1 + 1.44\left[1 - \frac{1708(\sin^{1.6}(1.8Slope)}{Ra\cos(Slope)}\right] *$$

$$Max\left[0, \left(1 - \frac{1708}{Ra\cos(Slope)}\right)\right] +$$

$$Max[0, (\left(\frac{Ra\cos(Slope)}{5830}\right)^{1/3} - 1)]$$

$$Ra = Max\left[1, \left(\frac{g\,\Delta T_{plate}\,Spacing^3}{T_{plates}\vartheta_{fluid}\alpha_{fluid}}\right)\right]$$

$$\alpha_{fluid} = \frac{k_{fluid}}{\rho_{fluid} Cp_{fluid}}$$

If the flow in the channel is laminar (Reynolds number < 2300) then a constant surface temperature heat transfer is utilized:

$Nu = 3.66$

If the flow in the channel is turbulent (Reynolds number > 2300) the correlations by (Candanedo, 2010) are utilized.

The main thermal parameters used in the BIPV/T model are given in the table below.

Table 5: PV model thermal parameters.

PV/T channel height, m	PV substrate resistance, h.m^2.K/kJ	Absorptance of PV surface	Emissivity of PV surface	Back resistance, h.m^2.K/kJ
0.1	0.01	0.8	0.9	1.1028

Electrical output from the PV module is calculated using one diode equivalent circuit model of CS6P-260P PV module by Canadian Solar. The model is described in detail by (Eckstein, 1990) and (Duffie & Beckman, 2006). The electrical output is used at maximum power point. The potential capacity of the BIPV and BIPV/T integrated in the spandrel section of the analyzed perimeter zone and consists of 18 PV panels for 0.5 whole south curtain wall façade per one floor, which results in a total of 4.42 kW of nominal PV power if 260 W PV panels described below are used.

The overhang effect on the building loads is estimated using the methodology described in (Klein et al., 2012). The effect of façade with PV overhangs self-shading from overhangs installed above one another is taken into account as well. This effect can result in PV module overall efficiency decrease, since the shading is significant during the summer days, when the solar altitude angle is high. Shaded PV cells result in reduced power output of the PV string, since the string current drops to the shaded cell current. Shading of PV cells also results in hot spots on the PV cells, which can result in damage of the modules in the long term due to thermal stress. The algorithm how to estimate the string shading is described in (Duffie & Beckman, 2006) and (Thornton et al., 2012).

PV shutter is a PV panel acting as an opaque shading device in front of the top window section. It is implemented in the building model as an exterior shading device blocking 100% of the incoming solar radiation to the space through the top window and adding additional thermal resistance of 0.0714 h-m^2-K/kJ to this glazing section. The installed capacities of PV shading devices for 0.5 south perimeter zone per floor are given in the table below.

Table 6: Shading devices with PV properties.

	Overhangs			Shutter
Device width, m	0.51	1.01	1.50	0.97
PV length, m	3.15	3.15	3.15	1.66
Tilt angle, degrees	8	6	3	90
Amount of PV shades per analyzed perimeter zone	4	8	12	8
Installed PV capacity, kW	1.04	2.08	3.12	2.08

One-diode equivalent circuit model of CS6P-260P PV module by Canadian Solar was used to calculate the performance of the PV overhangs and PV solar shutters. The needed shading device dimensions in the model are not the same as the CS6P-260P. For this purpose the dimension variations of the CS6P-260P panel were assumed to not affect the electrical performance of the PV module as long as the area of the module and number of cells were kept the same.

The PV/T-air collector integrated in façade is a framed PV air-based solar thermal collector. The framing system allows the air collectors to be installed using conventional curtain wall construction elements and PV modules act as a spandrel section cladding elements. The PV modules generate electricity and warm air, while performing as a rain screen cladding with high architectural integration flexibility. Conventional silicon technology PV panels have a lifetime of nearly 30 years, which offers durability of a conventional metal cladding material.

The hybrid BIPV/T assisted ventilation case delivers the preheated air directly to the perimeter zone, when the adequate temperature outlet air is available. The designed system shows potential in reducing the cooling or heating demand during the sunny heating season days, when the outdoor air needs to be preheated in the air handling system, before being delivered to the zone. The basic design is shown in figure below. Variable speed fan is operated as follows:

- Fan startup initiated if BIPV/T outlet temperature difference with room heating

setpoint is above -2 ^{o}C. Otherwise, the fan is OFF;

- Mass flow rate has an exterior temperature based mass flow reset. If ambient temperature (T_{amb}) is below or equal than -10 ^{o}C, exterior air reset (EAR) is 0.5. If -10<T_{amb}<=0, then EAR is 0.8. If T_{amb}>1, then EAR is 1. The effective mass flow rate is 6.9 L/s-m^2;
- The fan is OFF, if relative humidity is above 80% or below 20%;
- Anticipated overheat protection turns off the fan if the output of BIPV/T is above 25 ^{o}C and T_{amb} is above 16 ^{o}C;
- In this case economizer was modeled and a 6.9 L/s-m^2 mass flow rate was enabled if 13<T_{amb}<=22 ^{o}C;
- Also in this case the nighttime cooling was enabled between May-September, which allowed outdoor air at 4.33 L/s-m^2 if the T_{amb}>=13 ^{o}C during nighttime and relative humidity is between 20 and 80%.

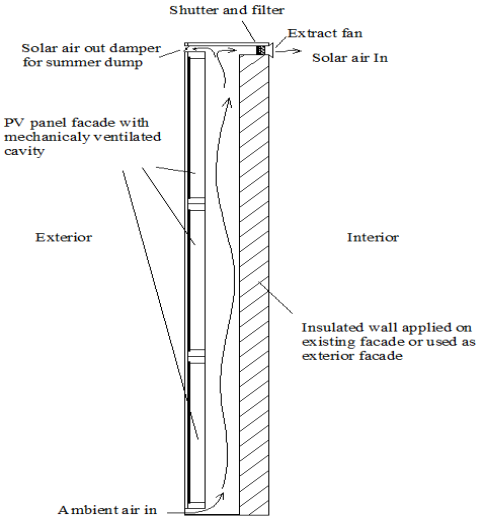

Figure 5: BIPV/T wall element used for hybrid BIPV/T assisted ventilation case.

The values proposed for the fan mass flow rate reset control strategy were optimized based on developed model best annual performance and should be tuned for each building category separately. Also, care must be taken, when using high supply mass flow rates, which can result in draughts and uncomfortable conditions in the space as a result. The focus of this analysis is the potential of these systems from energy saving point of view, having in mind that the high mass flow rate air supply will be active only for short period of time, when the solar irradiation is highest, thus BIPV/T output is useful for space conditioning, when simultaneously the cooling load is the highest.

RESULTS

ENVELOPE RETROFIT POTENTIAL

Extensive (over 140) simulation runs varying façade insulation levels, glazing U-value and WWR for south and west facade of the whole building model were performed to develop the energy use intensity (EUI) and Energy saving over Investment (kWha/$) ratio matrixes for the case study building. See figures 6 and 7.

As observed from the simulation results replacement of glazing from a U-value of 3.52 W/m^2-^{o}C to 2.16 W/m^2-^{o}C results in EUI drop by 6% for the same façade thermal resistance value. Change of façade thermal resistance from RSI 0.88 to RSI 6 results in a 23% drop for current WWR (48%), 26% for the case with reduced WWR (30%) and 29% for the case with WWR (20%). The lowest EUI value achieved is 238 kWh/m^2-yr for the case with RSI 6, 20% WWR for the south and west facades and glazing U value 2.16. South and west façade window opening area redesign benefits would be 2% for 30% WWR and 3% for 20% WWR for the same RSI value. In the case of RSI 2.5, EUI drop from 295 kWh/m^2-yr to 282 kWh/m^2-yr and to 277 kWh/m^2-yr (or 4% and 5% EUI drop respectively) for the same south and west façade WWR redesign cases occurs. Decrease in glazing U value from 3.52 W/m^2-^{o}C to 3.04 W/m^2-^{o}C with SHGC of 0.62 results in EUI decrease by 2%. Changing the glazing from 3.52 W/m^2-^{o}C with 0.62 SHGC to 2.39 with 0.5 SHGC results in EUI decrease only by 1% or none at all in cases with reduced WWR. Replacement of glazing with a glazing having U value of 2.16 W/m^2-^{o}C and SHGC of 0.5 results in EUI reduction of 3% for the case with 43% WWR and of 1% for the cases with reduced WWR for the same insulation level.

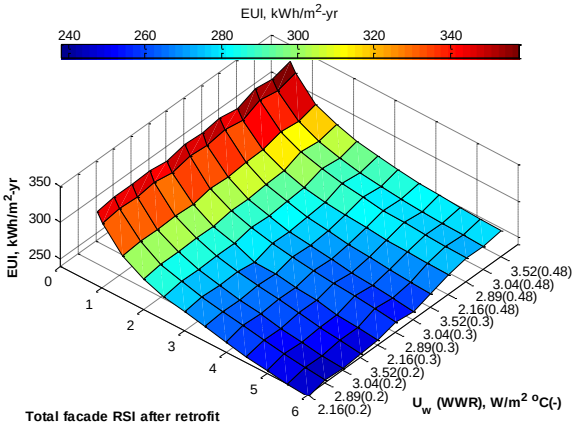

Figure 6: EUI vs. façade retrofit measures matrix.

Energy savings for the first year in kWh ratio to investment in $ is estimated based on current material

prices as described in the previous section. This ratio is proposed to identify the most attractive facade retrofit combination. For the case studied the energy savings over investment ratios are highest for the case when additional RSI from 1.2 to 1.7 is applied for the same glazing values. This case is attractive for both existing south and west glazing areas and with reduced WWR to 20%. Reduction to 30% is also peaking for this case, but at a 7% lower rate than with existing WWR.

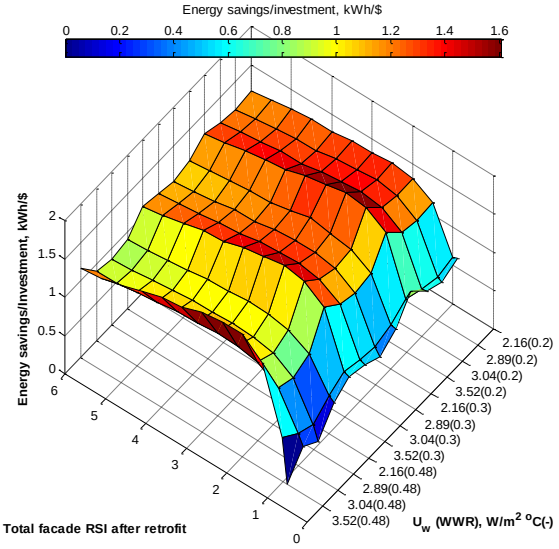

Figure 7: Energy saving/investment vs. façade retrofit measures matrix.

In the case, when it is identified, that replacement of glazing is necessary, it is observed, that the best case could be both redesigning the south and west facades to lower WWR, increasing the RSI by 2.2 (total of RSI 3 for this case) and replacing the glazing with either slightly higher insulating value, but higher SHGC (3.04 W/m2-ºC and 0.62 SHGC) or considerably higher insulating value if the SHGC are lower than the base case (2.16 W/m2-ºC with 0.5 SHGC).

SOLAR SYSTEM POTENTIAL

A perimeter zone model with GFA is 65 m^2 based on the validated full scale model was created to analyze the façade integrated solar system effect on the south and west perimeter zone in a higher resolution. The lighting load is estimated using radiosity model. Results are given for the south perimeter zone only.

12 cases were simulated. C1 is the base case, C2 is with increased opaque section thermal resistance to RSI 2.5, C3 – add to the previous measure windows were replaced to ones with U=2.16 W/m2-ºC and SHGC=0.5, C4 – case C3 plus an 0.5 m overhang above the daylighting section of the three section curtain wall facade with installed 0.161 kW/m^2 capacity PV system, C5 – case C3 with 1 m overhang and the same PV system capacity, C6 – case C3 with 1.5 m overhang and the same PV system capacity. C7 is the same as case C5, but the overhang is placed above vision section and the daylighting section is not obstructed. C8 the same as case C7, but the vision section is replaced with opaque section, and additionally a nighttime shutter added (case C9). C10 – is as case C3 plus the top glazing section blocked with an opaque vertical PV panel. C11 is as case C3 plus a naturally ventilated BIPV spandrel with installed 0.155 kW/m^2 capacity PV system and C12 is as case C9 (excluding the overhang) plus the BIPV/T system described in the previous chapter. The simulation results are shown in the figure 8.

As visible from simulation results, to achieve a nearly net zero perimeter zone even on south facing orientation requires further optimization, which includes demand side measures, efficient HVAC systems, like radiant systems with storage. On the other hand, even with existing HVAC and interior space plan the façade redesign measures can lead to significant savings in energy consumption. External shading system (overhang with PV) results in electricity generation of 19.6 kWh/m^2 to 53 kWh/m^2 for the perimeter zone floor area or 849 kWh/kWp and cooling load decrease by nearly 40%, but the total benefit is diminished by increased heating and lighting load. Increase of opaque area on the façade decreases the total energy consumption by another 5% (case C7). Case C10 demonstrates 53% reduction comparing to base case C1 and 10-15% better performance than overhang system. The case C11 shows the potential of addition of spandrel BIPV from energy generation point of view and C12 demonstrates the energetic potential of BIPV/T system with direct fresh air intake to perimeter zone space + nighttime ventilation, which results in 36% reduction in cooling load, 59% reduction in heating load and additional 92.65 kWh/m^2-yr for the perimeter zone floor area or 1293 kWh/kWp.

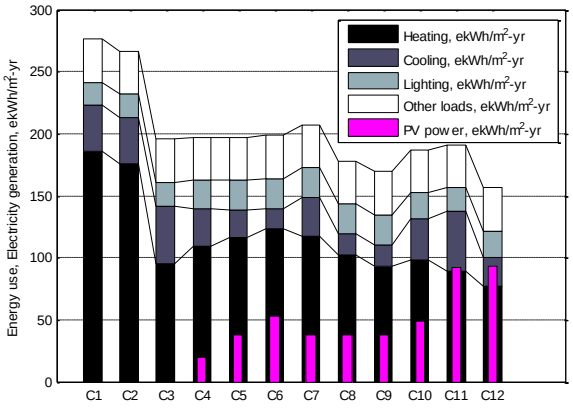

Figure 8: South perimeter zone simulation results.

Cases with roof installation and areas R and L (refer to figure 4), were not considered for the perimeter zone analysis due to low influence on perimeter zone thermal performance, but are taken into consideration in further analysis.

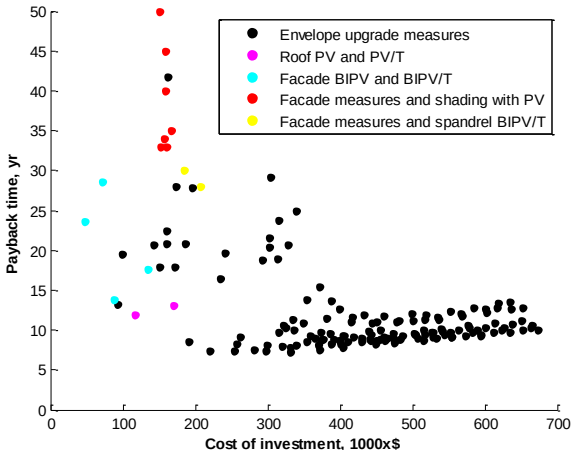

Figure 9: Scatter plot of payback time vs. Cost of investment of a retrofit mean or solar system.

As a final step, payback time and net present value (NPV) of the analysed retrofit cases for 30 years were plotted over cost of investment. Payback times are attractive for envelope retrofit for this case due to low initial RSI value. Addition of solar systems seems the most feasible in the case of roof mounted PV and PV/T systems, due to lower delivery costs. Spandrel integrated BIPV and BIPV/T demonstrates relatively the same payback times as roof mounted PV rack system, due to higher integration and delivery costs, but with additional benefits related to façade retrofit (like increased building value, etc.). The lowest payback times are for the shading systems.

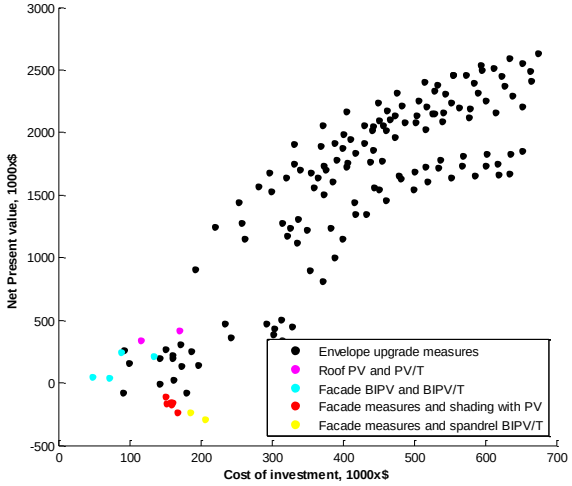

Figure 10: Scatter plot of net present value of proposed retrofit approaches and systems after 30 years vs. cost of investment.

The NPV plot vs. cost of investment provides an estimate of what is the expected total monetary value to the building owner of each system in 30 years. The integrated systems start generating revenue to the building owner later than the conventional envelope retrofit measures, since the façade retrofit is considered only for the south and west facades, which reduces the total energy saving annual portion. The cases which are negative can be considered as risky investment. The only way to increase the potential and applicability of these technologies is reduction of delivery costs, which comes through larger scale manufacturing, prefabrication, incentives etc.

CONCLUSION

Retrofit design potential analysis was carried out, looking into a medium size office building in Saskatoon climate, to identify the potential of façade retrofit and redesign combinations taking into account façade-integrated solar systems in an urban area. This analysis was done for a building with 7.6 m deep perimeter zones and large core (perimeter floor area 33% larger than core). For the case study building, it was observed, that through façade retrofit measures, the EUI can be reduced from 366 kWh/m^2-yr to 231 kWh/m^2-yr by increasing the façade RSI by 5.8 up to RSI, with glazing replacement from base case to 2.16 W/m^2-^{o}C with 0.5 SHGC and WWR reduction to 20%. For a basic estimation of the most cost effective case a ratio of Energy savings over Investment (kWh/$) was used. As observed, the most cost-effective cases were when additional RSI from 1.2 to 1.7 is applied with the existing glazing U values or if the replacement of glazing is necessary, both

redesigning the south and west facades to lower WWR, increasing the RSI by 2.2 (total of RSI 3 for this case) and replacing the glazing with either slightly higher insulating value, but higher SHGC (3.04 W/m2-ºC and 0.62 SHGC) or considerably higher insulating value if the SHGC are lower than the base case (2.16 W/m2-ºC with 0.5 SHGC).

The perimeter zone model with integrated solar system and daylighting algorithms, demonstrated that the case with façade redesign and spandrel integrated BIPV/T system can lead to reduction in heating load by 59%, cooling load by 46% with only 15% increase in lighting load with additional 92.65 kWh/m^2-yr for the perimeter zone floor area or 1293 kWh/kWp, which could cover 86% of the south façade perimeter zone electricity needs in Saskatoon climate. This case demonstrates payback times 1-3 years higher than PV rack system on the roof. Shading systems with PV energy generation potential from 19 kWh/m^2-yr to 53.15 kWh/m^2-yr or 849 kWh/kWp for south façade.

Super insulating non-residential buildings are not considered, due to observed optimal amount of additional insulation by RSI 1.2-2.2 for this case up to total of RSI 3. Other measures, like demand side measures, occupancy related control, higher solar heat and light utilization, more efficient HVAC, mechanical equipment and operation strategies should be used, when dropping the EUI value to lower ranges for opportunities to reach nearly net zero office building performance.

Future work includes further analysis on occupant comfort indices, other energy efficiency measures, benchmarking of the most promising solar façade designs and development of a retrofit toolkit.

ACKNOWLEDGEMENTS

The authors acknowledge the support of the Natural Sciences and Engineering Research Council of Canada (NSERC) through the Smart Net-zero Energy Buildings Strategic Research Network and one of its partners – the City of Saskatoon.

NOMENCLATURE

CDD – *cooling degree days*
c_{pfluid} – *specific heat capacity or air, kJ/kg-K*
CV-RMSE – root mean square error coefficient of variation, %
ΔT_{plate} – *temperature difference between air collector plates, K*
g – *acceleration due to gravity, m/s*^{2}
HDD – *heating degree days*
k_{fluif} – *thermal conductivity of air, kJ/hr-m-K*
NMBE – *normalized mean biased error, %*
NU – *Nusselt number*
Ra – *Rayleigh number*
ρ_{fluid} – *density of air, kg/m*^{3}
Slope – *slope of BIPV/T collector, degrees*
Spacing – BIPV/T air channel gap thickness, m
ϑ_{fluid} – *viscosity of the air, kg/m-hr*

REFERENCES

Bambara, J., Athienitis, A. K., & O'Neill, B. (2011). Design and Performance of a Photovoltaic/Thermal System Integrated with Transpired Collector. *ASHRAE Transactions, 117*.

Bobinson, D., Haldi, F., Kampf, J., & Leroux, P. (2009). *CITYSIM: Comprehensive micro-simulation of resource flows for sustainable urban plannin*. Paper presented at the Eleventh International IBPSA Conference, Glasgow, Scotland.

Boma Best. (2015). *5. Module Definitions an Performance Benchmarks.* Boma Best Application Guide.

Candanedo, L. (2010). *Modelling and Evaluation of the Performance of Building-Integrated Open Loop Air-based Photovoltaic/Thermal Systems.* (PhD), Concordia University, Montreal, Canada.

Chen, Y. (2013). *Methodology for Design and Operation of Active Building-Integrated Thermal Energy Storage Systems.* (PhD), Concordia University, Montreal, Canada.

Christensen, C., Anderson, R., Horowitz, S., Courtney, A., & Spencer, J. (2006). *BEopt Software for building energy optimization: features and capabilities* (NREL/TP-550-39929). U.S. Department of Energy, National Renewable Energy Laboratory.

Duffie, J. A., & Beckman, W. A. (2006). *Solar Engineering of Thermal Processes*. New Jersy: John Wiley & Sons.

Eckstein, J. H. (1990). *Detailed Modeling of Photovoltaic Components.* (M. S. Thesis), University of Wisconsin, Madison.

Eisenhower, B., O'Neill, Z., Narayanan, S., Fonoberov, V. A., & Mezić, I. (2012). A methodology for meta-model based optimization in building energy models. *Energy and Buildings, 47*, 292-301. doi:http://dx.doi.org/10.1016/j.enbuild.2011.12.001

Esclapés, J., Ferreiro, I., Piera, J., & Teller, J. (2014). A method to evaluate the adaptability of photovoltaic energy on urban façades. *Solar Energy, 105*, 414-427.

doi:http://dx.doi.org/10.1016/j.solener.2014.03.012

Fuentes, M. (2007). *Integration of PV into the built environment*. Brita in PuBs - Bringing retrofit innovation to application in public buildings. EU 6th framework program Eco-building. London, UK.

Gnanam, B. (2013). *Smart Energy Suburbs: Retrofitting Suburban Communities*. Paper presented at the Quest 2013: Integrated Energy Solutions for Everyday Community. Conference and Tradeshow Markham, Ontario.

Gugliermetti, F., & Bisegna, F. (2006). Daylighting with external shading devices: design and simulation algorithms. *Building and Environment, 41*(2), 136-149. doi:http://dx.doi.org/10.1016/j.buildenv.2004.12.011

Guiavarch, A., & Peuportier, B. (2006). Photovoltaic collectors efficiency according to their integration in buildings. *Solar Energy, 80*, 65-77.

Halverson, M., Rosenberg, M., Wang, W., Zhang, J., Mendon, V., & Athalye, R. (2014). ANSI/ASHRAE/IES Standard 90.1-2013 Preliminary Determination: Quantitative Analysis. U.S. Department of Energy under Contract DE-AC05-76RL01830.

Hastings, S. R. (1999). *Solar Air Systems: Built Examples*. New York: James & James.

Henning, H.-M., & Doll, J. (2012). Solar systems for heating and cooling of buildings. *Energy Procedia, 30*, 633 - 653.

Heo, Y., Choudhary, R., & Augenbroe, G. A. (2012). Calibration of building energy models for retrofit analysis under uncertainty. *Energy and Buildings, 47*, 550-560. doi:http://dx.doi.org/10.1016/j.enbuild.2011.12.029

IEA. (2014). SCH Task 47: Solar Renovation of Non-Residential Buildings.

Jensen, S. O. (2001). *Results from measurements on the PV-VENT systems at Lundebjerg. Report*. Danish Technological Institute, Solar Energy Centre. PV-VENT project report under JOULE.

Kirimtat, A., Koyunbaba, B. K., Chatzikonstantinou, I., & Sariyildiz, S. (2016). Review of simulation modeling for shading devices in buildings. *Renewable and Sustainable Energy Reviews, 53*, 23-49. doi:http://dx.doi.org/10.1016/j.rser.2015.08.020

Klein, S. A., Beckmn, W. A., Mitchell, J. W., & Duffie, J. A. (2012). *Trnsys 17. Volume 4 Mathematical Reference of standard components.* Solar Energy Laboratory, University of Wisconsin-Madison, Madison, U.S.A.

Lai, C.-M., & Hokoi, S. (2015). Solar façades: A review. *Building and Environment, 91*, 152-165. doi:http://dx.doi.org/10.1016/j.buildenv.2015.01.007

Lechner, N. (2014). *Heating, Cooling, Lighting. Sustainable methods for architects.* New Jersey, The USA: Wiley.

Lee, S. H., Hong, T., Piette, M. A., & Taylor-Lange, S. C. (2015). Energy retrofit analysis toolkits for commercial buildings: A review. *Energy, 89*, 1087-1100. doi:http://dx.doi.org/10.1016/j.energy.2015.06.112

Martinez, A., & Carlson, A. (2014). *State of the Art Methodology to Assess Energy Facade Retrofits*. Paper presented at the ARCC/EAAE 2014: Beyond Architecture: New Intersections & Connections.

Martinez, A., Patterson, M., Carlson, A., & Noble, D. (2015). Fundamentals in Façade Retrofit Practice. *Procedia Engineering, 118*, 934-941. doi:http://dx.doi.org/10.1016/j.proeng.2015.08.534

Mattei, M., Notton, G., Cristofari, C., Muselli, M., & Poggi, P. (2006). Calculation of the polycrystalline PV module temperature using a simple method of energy balance. *Renewable Energy, 31*(4), 553-567. doi:http://dx.doi.org/10.1016/j.renene.2005.03.010

Maurer, C., & Kuhn, T. E. (2012). Variable g value of transparent façade collectors. *Energy and Buildings, 51*, 177-184. doi:http://dx.doi.org/10.1016/j.enbuild.2012.05.011

Mei, L., Infield, D., Eicker, U., Loveday, D., & Fux, V. (2006). Cooling potential of ventilated PV façade and solar air heaters combined with a desiccant cooling machine. *Renewable Energy, 31*(8), 1265-1278. doi:http://dx.doi.org/10.1016/j.renene.2005.06.013

Márquez-García, A., Varo-Martínez, M., & López-Luque, R. (2013). Toolbox engineering software for the analysis of sunlight on buildings. *International Journal of Low-Carbon Technologies*. doi:10.1093/ijlct/ctt062

NRCan-OEE. (2013). *Survey of Commercial and Institutional Energy Use - Buildings 2009*

(Detailed Statistical Report March 2013). Natural Resources Canada, Ottawa:

NRTEE. (2009). *Geared for Change: Energy Efficiency in Canada's Commercial Building Sector*. Ottawa.

Quesada, G., Rousse, D., Dutil, Y., Badache, M., & Hallé, S. (2012). A comprehensive review of solar facades. Opaque solar facades. *Renewable and Sustainable Energy Reviews, 16*(5), 2820-2832. doi:http://dx.doi.org/10.1016/j.rser.2012.01.078

Redweik, P., Catita, C., & Brito, M. (2013). Solar energy potential on roofs and facades in an urban landscape. *Solar Energy, 97*, 332-341. doi:http://dx.doi.org/10.1016/j.solener.2013.08.036

Robinson, D., Campbell, N., Gaiser, W., Kabel, K., Le-Mouel, A., Morel, N., Stone, A. (2007). SUNtool – A new modelling paradigm for simulating and optimising urban sustainability. *Solar Energy, 81*(9), 1196-1211. doi:http://dx.doi.org/10.1016/j.solener.2007.06.002

Rysanek, A. M., & Choudhary, R. (2013). Optimum building energy retrofits under technical and economic uncertainty. *Energy and Buildings, 57*, 324-337. doi:http://dx.doi.org/10.1016/j.enbuild.2012.10.027

Saranti, A., Tsoutsos, T., & Mandalaki, M. (2015). Sustainable Energy Planning. Design Shading Devices with Integrated Photovoltaic Systems for Residential Housing Units. *Procedia Engineering, 123*, 479-487. doi:http://dx.doi.org/10.1016/j.proeng.2015.10.099

Sarralde, J. J., Quinn, D. J., Wiesmann, D., & Steemers, K. (2015). Solar energy and urban morphology: Scenarios for increasing the renewable energy potential of neighbourhoods in London. *Renewable Energy, 73*, 10-17. doi:http://dx.doi.org/10.1016/j.renene.2014.06.028

Silva, P. C. P., Almeida, M., Bragança, L., & Mesquita, V. (2013). Development of prefabricated retrofit module towards nearly zero energy buildings. *Energy and Buildings, 56*, 115-125. doi:http://dx.doi.org/10.1016/j.enbuild.2012.09.034

Thornton, J. W., Bradley, D. E., McDowell, T. P., Blair, N. J., & Duffy, M. J. (2012). *Electrical Library mathematical Reference. TESSLibs17*. Component Libraries for the TRNSYS Simulation Environment. Solar Energy Laboratory, University of Wisconsin - Madison.

Tregenza, P. (1987). Subdivision of the sky hemisphere for luminance measurements. *Lighting Research and Technology, 19*, 13-14.

Tzempelikos, A., & Athienitis, A. K. (2007). The impact of shading design and control on building cooling and lighting demand. *Solar Energy, 81*(3), 369-382. doi:http://dx.doi.org/10.1016/j.solener.2006.06.015

U.S. DOE. (2015). Energy Plus. http://apps1.eere.energy.gov/buildings/energyplus/: U.S. Department of Energy & NREL.

van Dijk, H., Spiekman, M., & de Wilde, P. (2005). *A monthly method for calculating energy performance in the context of European building regulations*. Paper presented at the Ninth International IBPSA Conference, International Building Performance Simulation Association, Montreal, Canada.

van Moeseke, G., Bruyère, I., & De Herde, A. (2007). Impact of control rules on the efficiency of shading devices and free cooling for office buildings. *Building and Environment, 42*(2), 784-793. doi:http://dx.doi.org/10.1016/j.buildenv.2005.09.015

Voss, K. (2000). Solar energy in building renovation - results and experience of international demonstration buildings. *Energy and Buildings, 32*, 291-302.

Zhang, X., Shen, J., Lu, Y., He, W., Xu, P., Zhao, X., . . . Dong, X. (2015). Active Solar Thermal Facades (ASTFs): From concept, application to research questions. *Renewable and Sustainable Energy Reviews, 50*, 32-63. doi:http://dx.doi.org/10.1016/j.rser.2015.04.108

Zondag, H. (2008). Flat-plate PV-Thermal collectors and systems: A review. *Renewable & Sustainable Energy Reviews*, 891-959.